

## CANCER

# Two-step enhanced cancer immunotherapy with engineered *Salmonella typhimurium* secreting heterologous flagellin

Jin Hai Zheng,<sup>1,2</sup> Vu H. Nguyen,<sup>1,3</sup> Sheng-Nan Jiang,<sup>4,5</sup> Seung-Hwan Park,<sup>6</sup> Wenzhi Tan,<sup>7</sup> Seol Hee Hong,<sup>8</sup> Myung Geun Shin,<sup>9</sup> Ik-Joo Chung,<sup>10</sup> Yeongjin Hong,<sup>7</sup> Hee-Seung Bom,<sup>4</sup> Hyon E. Choy,<sup>2,7</sup> Shee Eun Lee,<sup>8</sup> Joon Haeng Rhee,<sup>2,7\*</sup> Jung-Joon Min<sup>1,2,4,7\*</sup>

2017 © The Authors,  
some rights reserved;  
exclusive licensee  
American Association  
for the Advancement  
of Science.

We report a method of cancer immunotherapy using an attenuated *Salmonella typhimurium* strain engineered to secrete *Vibrio vulnificus* flagellin B (FlaB) in tumor tissues. Engineered FlaB-secreting bacteria effectively suppressed tumor growth and metastasis in mouse models and prolonged survival. By using Toll-like receptor 5 (TLR5)-negative colon cancer cell lines, we provided evidence that the FlaB-mediated tumor suppression upon bacterial colonization is associated with TLR5-mediated host reactions in the tumor microenvironment. These therapeutic effects were completely abrogated in TLR4 and MyD88 knockout mice, and partly in TLR5 knockout mice, indicating that TLR4 signaling is a requisite for tumor suppression mediated by FlaB-secreting bacteria, whereas TLR5 signaling augmented tumor-suppressive host reactions. Tumor microenvironment colonization by engineered *Salmonella* appeared to induce the infiltration of abundant immune cells such as monocytes/macrophages and neutrophils via TLR4 signaling. Subsequent secretion of FlaB from colonizing *Salmonella* resulted in phenotypic and functional activation of intratumoral macrophages with M1 phenotypes and a reciprocal reduction in M2-like suppressive activities. Together, these findings provide evidence that nonvirulent tumor-targeting bacteria releasing multiple TLR ligands can be used as cancer immunotherapeutics.

## INTRODUCTION

Abnormal blood vessels and hypoxic and necrotic regions are universal features of solid tumors (1, 2). These hypoxic and anoxic microenvironments may be targeted by obligatory or facultative anaerobic bacteria, such as *Bifidobacterium* (3), *Salmonella* (4, 5), *Escherichia* (6, 7), *Clostridium* (8), and *Listeria* (9). Such bacteria accumulate and actively proliferate within tumors, resulting in 1000 times or even higher increase in bacterial numbers in tumor tissues relative to those in normal organs such as liver and spleen (10). Recent studies of bacterial cancer therapy (BCT) show that several attenuated bacterial strains suppress tumor growth. VNP20009, an attenuated strain of *Salmonella typhimurium* with *purI* and *msbB* gene deletions, was safely administered to patients with metastatic melanoma and renal cell carcinoma in a phase 1 study, where substantial tumor colonization was observed (11, 12). Another mutant strain, A1-R, inhibited the growth of various tumors in mouse models (13–15) and forced quiescent cells to enter the cell cycle, thereby making them sensitive to chemotherapy (16). We previously developed

an attenuated strain of *S. typhimurium*, which is defective in guanosine 5'-diphosphate-3'-diphosphate synthesis ( $\Delta$ ppGpp *S. typhimurium*), resulting in a 100,000- to 1,000,000-fold increased median lethal dose (LD<sub>50</sub>) (17). Different payloads have been used to increase the anticancer toxicity of the strains; for example, bacteria were engineered to express cytotoxic proteins such as cytolysin A (7, 18) and mitochondria-targeting apoptogenic moiety Noxa (19).

Different strategies have been used to deliver therapeutic agents, such as cytotoxic proteins (5, 7, 18), cytokines (20), antigens, and antibodies (21), or genetic materials, such as short hairpin RNA (22), to tumor tissues using engineered *Salmonella*. Of these, *Salmonella* strains expressing tumor inhibitory cytokines, such as interleukin-18 (IL-18) (20), LIGHT (23), or CCL21 (24), are promising tools for BCT, which would suppress tumor growth directly and/or by activating host immunity. Although these strategies resulted in improved therapeutic effects, they still have limitations; for example, multiple injections of bacteria are required, and tumors tend to recur (20, 23, 24).

Here, we engineered bacteria to overexpress and secrete a heterologous bacterial flagellin [*Vibrio vulnificus* flagellin B (FlaB)] and tested their effects in tumor-bearing mice. *V. vulnificus* express six flagellin structural genes (*flaA*, *flaB*, *flaF*, *flaC*, *flaD*, and *flaE*). Of these, FlaB appears to be the most crucial building block of the flagellar shaft (25) and is an excellent adjuvant for anticancer immunotherapy because it activates innate immune responses via the Toll-like receptor 5 (TLR5) signaling pathway (26).

The colonization and subsequent proliferation of  $\Delta$ ppGpp *S. typhimurium* within tumor tissues induce infiltration of immune cells, such as neutrophils and macrophages, which then secrete proinflammatory cytokines such as tumor necrosis factor- $\alpha$  (TNF- $\alpha$ ) and IL-1 $\beta$ , both of which contribute to anticancer effects (5, 27, 28). This inflammatory reaction is induced when TLR4 and the inflammasome are activated by both lipopolysaccharide (LPS) and damaged cancer cells (28). Secretion of FlaB by *Salmonella* within the tumor

<sup>1</sup>Laboratory of In Vivo Molecular Imaging, Institute for Molecular Imaging and Theragnostics, Chonnam National University Hwasun Hospital, Jeonnam 58128, Republic of Korea. <sup>2</sup>Department of Molecular Medicine (BrainKorea21 Plus), Chonnam National University Graduate School, Gwangju 61469, Republic of Korea. <sup>3</sup>Department of Experimental Therapeutics, Beckman Research Institute of City of Hope, Duarte, CA 91010, USA. <sup>4</sup>Department of Nuclear Medicine, Chonnam National University Medical School, Gwangju 61469, Republic of Korea. <sup>5</sup>Department of Nuclear Medicine, Affiliated Haikou Hospital, Xiangya School of Medicine, Central South University, Hainan 570-208, China. <sup>6</sup>Biological Resource Center, Korea Research Institute of Bioscience and Biotechnology, Jeongseup 56212, Republic of Korea. <sup>7</sup>Department of Microbiology and Clinical Vaccine R&D Center, Chonnam National University Medical School, Gwangju 61469, Republic of Korea. <sup>8</sup>Department of Pharmacology and Dental Therapeutics, School of Dentistry, Chonnam National University, Gwangju 61186, Republic of Korea. <sup>9</sup>Department of Laboratory Medicine, Chonnam National University Medical School, Gwangju 61469, Republic of Korea. <sup>10</sup>Department of Hemato-Oncology, Chonnam National University Medical School, Jeonnam 58128, Republic of Korea.

\*Corresponding author. Email: jimin@jnu.ac.kr (J.-J.M.); jhrhee@chonnam.ac.kr (J.H.R.)

microenvironment may further activate recruited immune cells through TLR5 signaling, thereby enhancing the secretion of tumor-suppressive effectors and amplifying the tumor-suppressive efficacy. An attenuated  $\Delta$ ppGpp *S. typhimurium* strain and its payload, FlaB, showed cooperative antitumor activity in mice, with no evidence of systemic toxicity. We also showed that this enhanced antitumor activity was mediated through a cooperative activation of TLR5 and TLR4 signaling pathways.

## RESULTS

### Engineering $\Delta$ ppGpp *S. typhimurium* to express FlaB

We used attenuated  $\Delta$ ppGpp *S. typhimurium* for the targeted delivery of the FlaB payload to tumor tissues. To generate an inducible vector system for bacterial expression of the therapeutic gene, we cloned the *flaB* gene into the pBAD plasmid vector in which the *pelB* leader sequence was fused to the upstream of *flaB* to guide extracellular secretion; gene expression from the plasmid [pBAD-*pelB*-FlaB (pFlaB)] was induced only in the presence of L-arabinose (Fig. 1A) (18, 29). Western blot analysis revealed the presence of FlaB protein (43 kDa) in both cell pellet and filtered culture supernatant from pFlaB-carrying bacteria after L-arabinose induction, whereas no FlaB protein was detected in the absence of L-arabinose (Fig. 1B). This result indicated that FlaB protein

expression was tightly regulated by L-arabinose and that the protein was successfully secreted from the bacteria that were guided by the *pelB* leader sequence, as observed previously (30).

### Evaluation of TLR5 expression in cancer cells and macrophages

FlaB acts via TLR5, which is expressed on the surface of various cells (31). To verify whether FlaB directly on cancer cells (31) or by activating host immune cells, we examined TLR5 expression in a mouse colon cancer cell line (MC38), a human colon cancer cell line stably expressing firefly luciferase (HCT116-luc2), and peritoneal macrophages, either on the surface or inside cells. TLR5 was not detected on the surface of MC38, and only a small percentage (about 2.5%) of HCT116-luc2 expressed TLR5 on the surface. However, macrophages were positive for TLR5 both on the surface and in the cytoplasm (Fig. 1C). These results indicate that tumor cells would not be directly affected by the TLR5 signaling, which was further confirmed again by the Western blot analysis and luciferase assay of nuclear factor  $\kappa$ B (NF- $\kappa$ B) activation (25). The in vitro stimulation of cancer cells with FlaB did not increase phosphorylation of NF- $\kappa$ B p65 (fig. S1) and luciferase reporter activities (fig. S2), suggesting that FlaB-mediated antitumor effects were not caused by direct action on cancer cells.

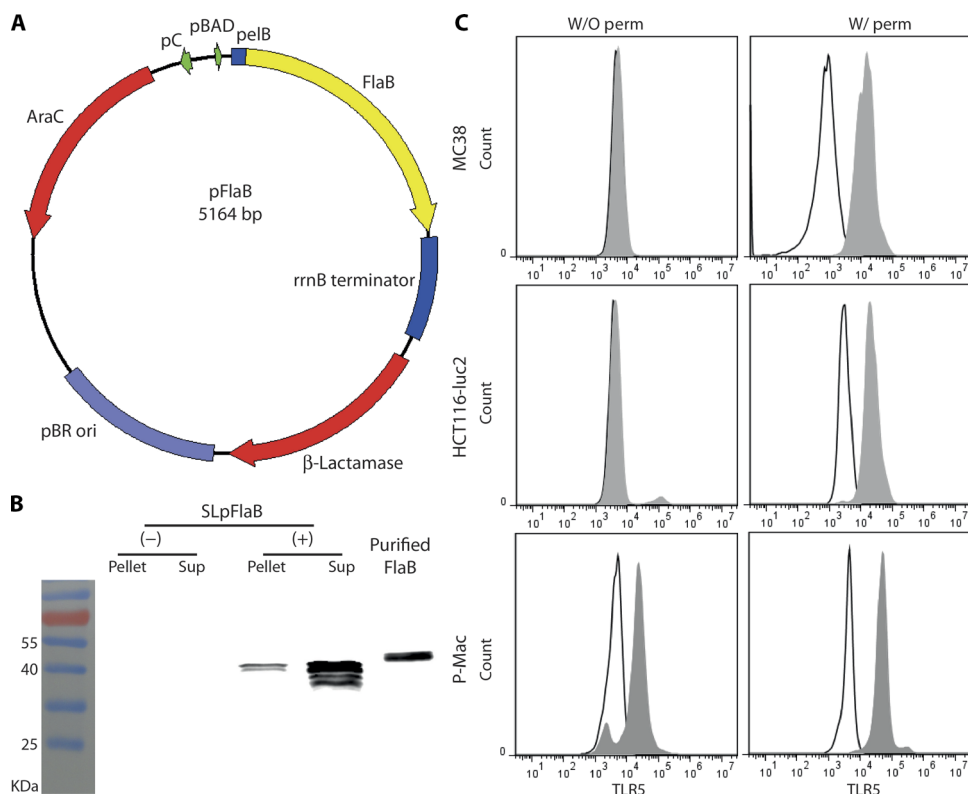


**Fig. 1. Engineering of FlaB-expressing bacteria and detection of TLR5 expression by cancer cells.** (A) Schematic map of the engineered plasmid pFlaB. bp, base pair. (B) Immunoblot analysis to check bacterial expression of FlaB in vitro. Samples were prepared with (+) or without (–) 0.2% L-arabinose and separated into pellet and supernatant (Sup) fraction. (C) Flow cytometry analysis of TLR5 expression in MC38, HCT116-luc2, and peritoneal macrophages (P-Mac) under nonpermeabilized and permeabilized conditions. Outlined peaks: isotype control; gray-filled peaks: stained with TLR5 antibody. Data are representative of more than three independent experiments ( $n = 5$ ). W/O perm, without permeabilization; W/ perm, with permeabilization.

### Bacterial accumulation and FlaB expression in tumor tissues

The selective accumulation and active proliferation of bacteria in tumor tissues should enable high expression of therapeutic genes within tumors with minimal toxicity to normal organs/tissues. We show that  $\Delta$ ppGpp *S. typhimurium* initially colonized the liver and spleen and induced splenomegaly, associated with increased numbers of neutrophils (figs. S3 and S4). The number of bacteria in the liver, spleen, and lung drastically decreased at 3 to 4 days post-inoculation (dpi), and bacteria began to proliferate preferentially in tumors, resulting in more than 10,000-fold higher numbers in tumor tissue than those in organs (figs. S5 to S7) (5, 18). Therefore, expression of therapeutic genes at this time point should cause minimal toxicity, if any, to normal tissues (fig. S8). Thus, we decided to administer L-arabinose to tumor-bearing mice at 3 dpi.

We observed a high number of bacteria [ $>10^{10}$  colony-forming units (CFU)/g] in MC38 tumors subcutaneously implanted in the flank of C57BL/6 mice after L-arabinose administration; there was no significant difference in bacterial numbers in tumors borne by mice in both L-arabinose induction and noninduction groups (Fig. 2A). We then examined expression of FlaB in implanted MC38 tumors treated with  $\Delta$ ppGpp *S. typhimurium* carrying pFlaB in the presence or absence

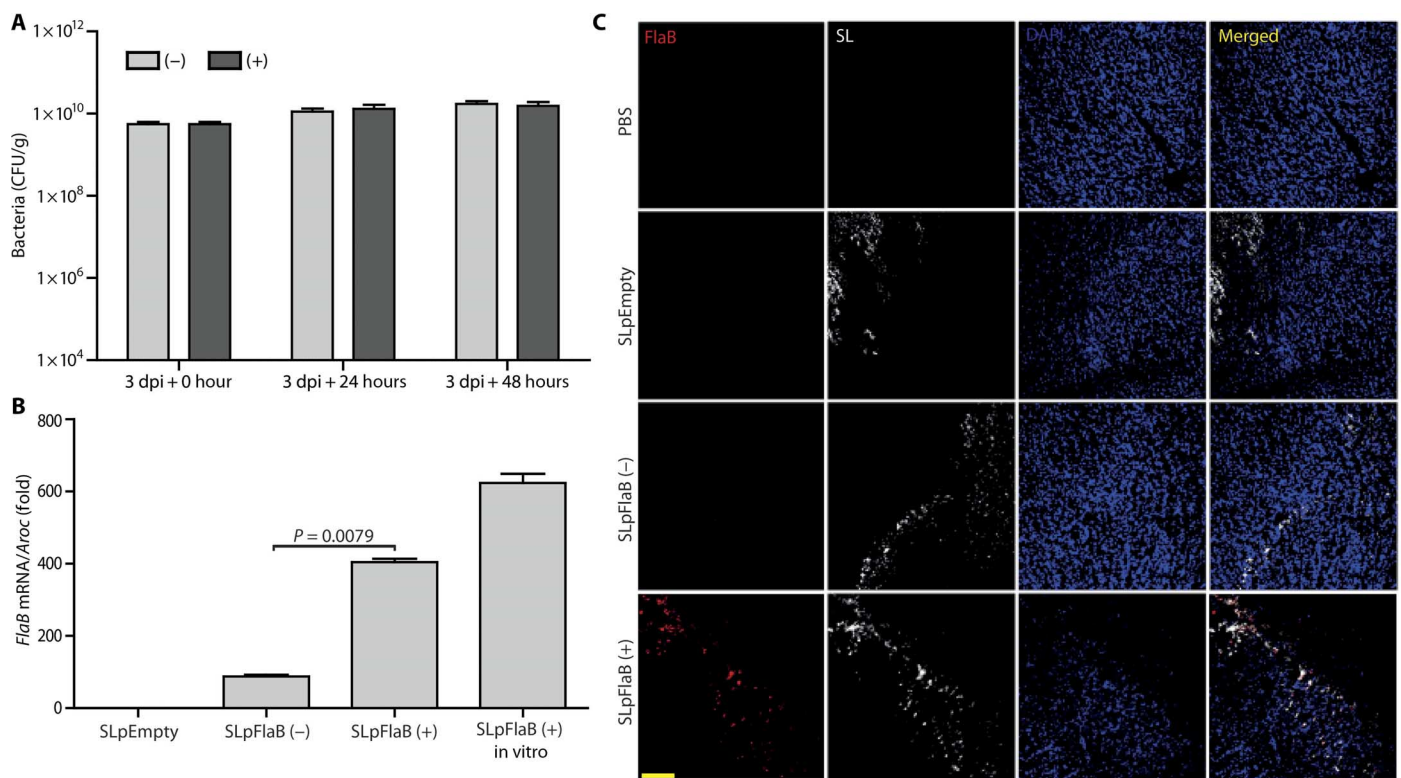


**Fig. 2. Bacterial colonization and FlaB expression in vivo.** (A) C57BL/6 mice ( $n = 11$ ) bearing MC38 tumors were intravenously injected with engineered FlaB-expressing *S. typhimurium* ( $1 \times 10^7$  CFU), followed by intraperitoneal injection of L-arabinose (daily, starting at 3 dpi). Viable bacteria were counted in tumors at 0, 24, and 48 hours after L-arabinose induction (or no induction). (B) Total bacterial mRNA ( $n = 9$ ) was isolated from tumor tissues infected with *S. typhimurium* carrying an empty vector (SLpEmpty) or *S. typhimurium* carrying FlaB (SLpFlaB) with (+) or without (-) L-arabinose induction (for 6 hours at 3 dpi). mRNA from in vitro-cultured SLpFlaB (+) was used as positive control. *flaB* mRNA was quantified by real-time reverse transcription PCR (RT-PCR) and normalized to the *aroC* housekeeping gene (data are expressed as the fold difference in expression). (C) Immunofluorescence staining of tumor sections prepared after 6 hours of induction at 3 dpi. Sections were stained with an anti-FlaB antibody (red) or an anti-*S. typhimurium* (SL) antibody (gray). Nuclei were stained with DAPI (4',6-diamidino-2-phenylindole) (blue). A merged image is also shown (Merged). Scale bar, 100  $\mu$ m. Data are representative of three independent experiments.

of L-arabinose. Control experiments used tumors treated with AppGpp *S. typhimurium* carrying an empty vector. Real-time polymerase chain reaction (PCR) of excised tumor tissue demonstrated that the expression of *flaB* mRNA in tumors colonized by bacteria was 400-fold higher than that of a housekeeping gene (*aroC*) in the presence of L-arabinose but was only 80-fold higher in the absence of L-arabinose. No *flaB* mRNA was detected in the tumor tissues of mice treated with *S. typhimurium* carrying the empty vector (Fig. 2B). Note that the positive control (L-arabinose-mediated induction of in vitro-cultured *Salmonella* carrying pFlaB) induced >600-fold increase in the *flaB* mRNA expression. We then performed immunofluorescence staining of tumor tissues to directly identify the FlaB protein. Histological analysis revealed abundant bacteria in tumor tissues in *Salmonella*-injected mice; no bacteria were observed in phosphate-buffered saline (PBS)-injected mice. The FlaB protein was detected only in tumor tissues harboring AppGpp *S. typhimurium* carrying pFlaB in the presence of L-arabinose (Fig. 2C and fig. S7). The FlaB expression coincided with the infiltration of AppGpp *S. typhimurium*. Together, the results confirmed that FlaB was being secreted in tumor tissues by the tumor-targeting engineered *S. typhimurium*.

### Tumor-suppressive effects of engineered bacteria secreting FlaB

C57BL/6 mice transplanted with MC38 or B16F10 tumors were injected intravenously with PBS, AppGpp *S. typhimurium* carrying an empty

vector, or AppGpp *S. typhimurium* carrying pFlaB (+/- L-arabinose induction) to evaluate the antitumor activity of engineered AppGpp *S. typhimurium*. A separate group received an intratumoral injection of purified FlaB, either with or without an intravenous injection of AppGpp *S. typhimurium* carrying an empty vector. The best therapeutic effect was observed in mice treated with *S. typhimurium* carrying pFlaB in the presence of L-arabinose: the tumor was no longer detectable in 11 of 20 (55%) mice at the experimental end point (Fig. 3A and figs. S9 and S10). We also observed markedly enhanced tumor suppression in mice that received a combination of *S. typhimurium* carrying an empty vector followed by an intratumoral injection of purified FlaB: three of eight treated mice (38%) showed complete tumor regression. Tumor shrinkage was significant in the bacteria-treated group in the absence of induction ( $P = 0.0002$ ), but the tumors tended to regrow. Similar to PBS treatment, intratumoral injection of purified FlaB did not suppress tumor growth in mice (Fig. 3, A and B). In addition, groups of animals that received engineered bacteria plus FlaB/arabinose, or bacteria plus intratumoral purified FlaB, survived longer than those in the other groups (Fig. 3C). Only mice showing complete tumor regression survived beyond day 52 after tumor challenge. These mice regrew the hair on the shaved right flank and remained healthy until observations ceased on day 120 (Fig. 3, A and C). These data suggest that FlaB within the tumor elicits antitumor activity only in the presence of *Salmonella*. This, along with the finding that FlaB alone had



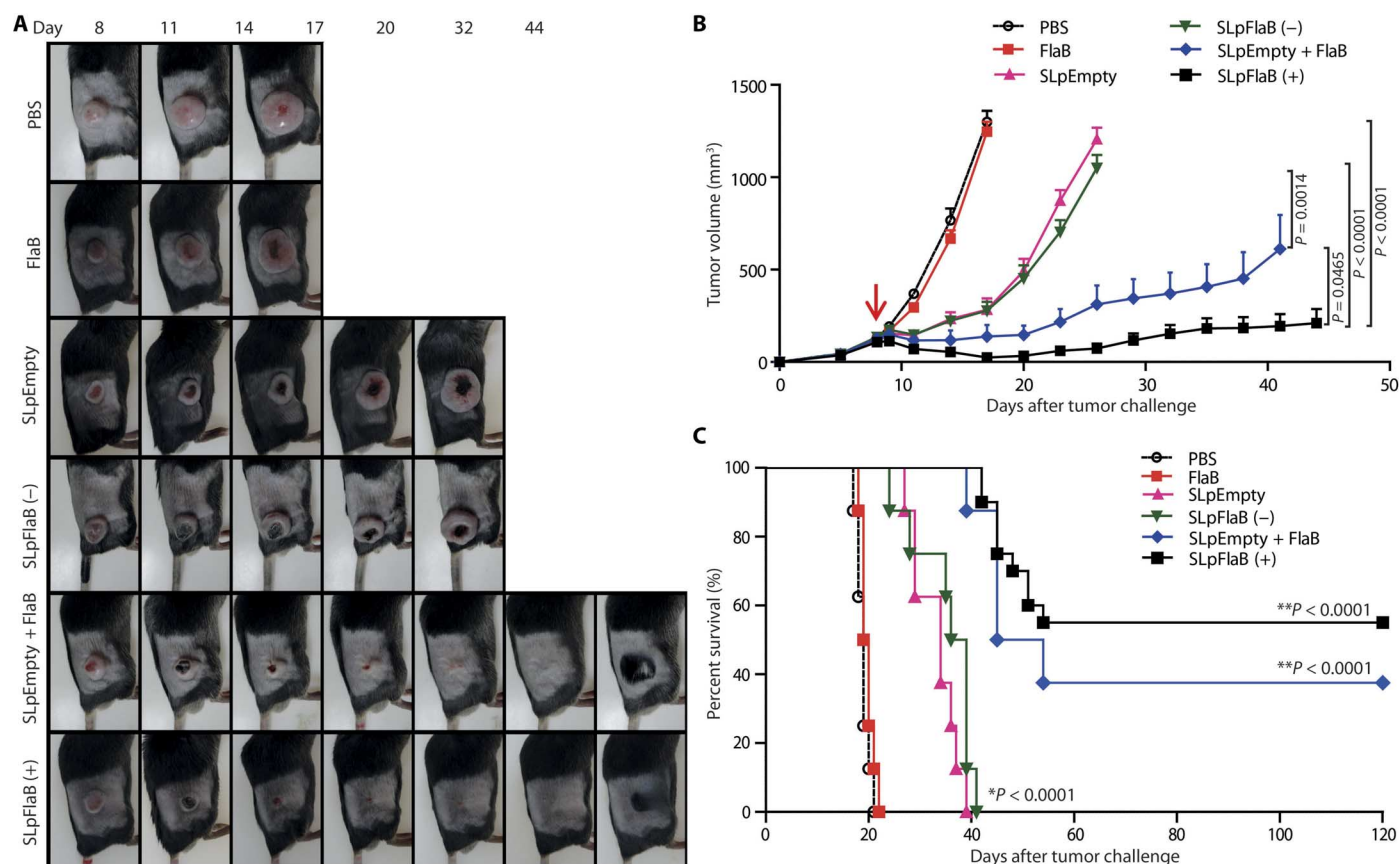


**Fig. 3. Effect of engineered FlaB-expressing *Salmonella* on growth and survival of MC38 tumors.** C57BL/6 mice ( $n = 8$  per group, except the SLpFlaB (+) group in which  $n = 20$ ) were subcutaneously injected with MC38 cells ( $1 \times 10^6$ ). When the tumors reached a volume of about 120 mm<sup>3</sup>, mice were divided into six treatment groups: PBS alone, purified FlaB alone, bacteria harboring pBAD-empty (pEmpty) (SLpEmpty), bacteria harboring pFlaB (SLpFlaB) either with (+) or without (-) L-arabinose induction, and bacteria harboring pEmpty plus intratumoral injection with purified FlaB (SLpEmpty + FlaB). Mice received ( $1 \times 10^7$  CFU) bacteria by intravenous injection (arrow). Where relevant, mice received 0.12 g of L-arabinose daily or an intratumoral injection of 2  $\mu$ g of purified FlaB every 2 days at 3 dpi. (A) Images of tumors from representative mice from each group. (B) Changes in tumor size. (C) Kaplan-Meier survival curves for MC38 tumor-bearing mice. Statistical significance was calculated by comparison with PBS or SL groups. \* $P < 0.0001$  (versus PBS group) and \*\* $P < 0.0001$  (versus SLpEmpty group).

no therapeutic effect, indicates that additional activation of TLR5 signaling in tumor tissue in which the microenvironment was modified in advance by *S. typhimurium* colonization is responsible for the enhanced tumor suppression. Notably, the tumor suppression activity of FlaB-secreting bacteria was superior to that of combination therapy comprising intravenous bacteria and intratumoral FlaB injections. The bacteria overgrown in tumor should have been secreting FlaB continuously in situ, which resulted in significantly enhanced destruction of tumor cells ( $P = 0.0465$ ) (Fig. 3).

### Enhanced effect of FlaB secretion from $\Delta$ ppGpp *S. typhimurium* on the metastasis of orthotopic human colon cancer in nude mice

To test whether the FlaB-secreting  $\Delta$ ppGpp *S. typhimurium* has inhibitory effects on human metastatic cancers, we next implanted HCT116-luc2 tumors into the intestinal wall of BALB/c athymic nu<sup>-</sup>/nu<sup>-</sup> mice using a surgical orthotopic implantation procedure. At day 4 after surgery, the tumor-bearing mice were divided into three treatment groups that received PBS (group 1; negative control),  $\Delta$ ppGpp *S. typhimurium* carrying an empty vector (group 2), and  $\Delta$ ppGpp *S. typhimurium* secreting FlaB (group 3). The FlaB-secreting

*S. typhimurium* significantly suppressed tumor metastasis ( $P < 0.0001$ ) (group 3; Fig. 4, A and B); only four metastatic lesions were generated in the peritoneal wall or intestine of three mice (Table 1). Compared with the control group, metastasis was also significantly inhibited in mice treated with *S. typhimurium* carrying an empty vector ( $P = 0.0017$ ) (Fig. 4, A and B); we found 26 lesions in group 2 and 91 lesions in group 1 (Table 1). The weight of the primary tumors in the group treated with the FlaB-secreting *S. typhimurium* was significantly lower than that in the group treated with empty vector-carrying *S. typhimurium* ( $P = 0.0158$ ) or the PBS group ( $P = 0.0085$ ) (Fig. 4C). These results indicate that FlaB-secreting bacteria inhibit primary tumor growth as well as metastasis in an orthotopic human cancer model.

### Role of host TLR signaling in the antitumor activity of FlaB-secreting *S. typhimurium*

Next, to determine whether the antitumor effects of FlaB-secreting  $\Delta$ ppGpp *S. typhimurium* were mediated through host TLR signaling, we compared its therapeutic efficacy in C57BL/6 wild type (WT) with that in TLR4<sup>-/-</sup>, TLR5<sup>-/-</sup>, or MyD88<sup>-/-</sup> mice. Growth of MC38 tumors in those knockout mice was similar to that in WT mice (fig. S11). When the engrafted MC38 tumors reached about 120 mm<sup>3</sup>, mice

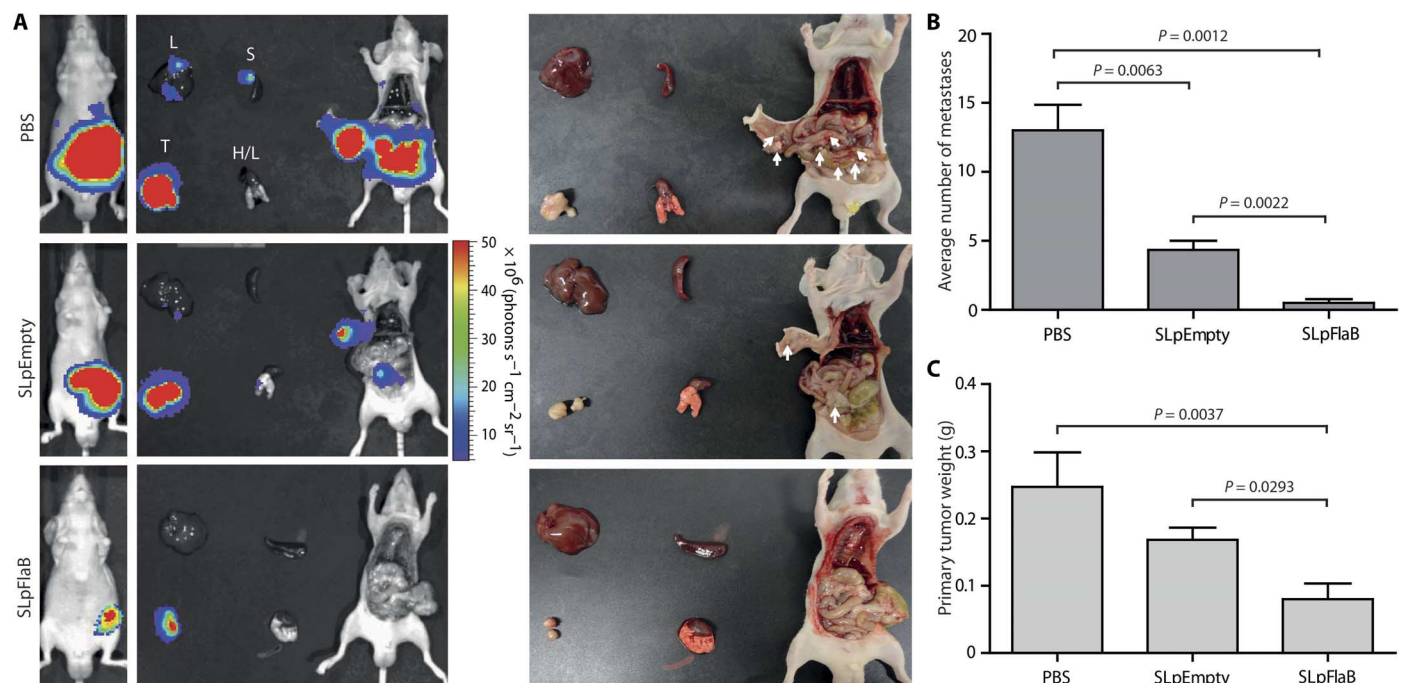


**Fig. 4. Effect of engineered FlaB-secreting *Salmonella* on orthotopic HCT116 human tumors in a nude mouse xenograft model.** BALB/c athymic  $\text{nu}^{-}/\text{nu}^{-}$  mice (PBS,  $n = 7$ ; SLpEmpty,  $n = 6$ ; SLpFlaB,  $n = 8$ ) were surgically implanted with two pieces of HCT116-luc2 tumor (each measuring  $1 \text{ mm}^3$ ) stably expressing firefly luciferase. Fragments were transplanted onto the ceca and ascending colon. Four days after surgery, mice were treated with PBS, bacteria harboring pEmpty (SLpEmpty), or bacteria harboring pFlaB with  $\text{l-arabinose}$  at 3 dpi (SLpFlaB). All animals were sacrificed at day 27 after transplantation. (A) Left: Bioluminescence images after intraperitoneal injection of  $750 \mu\text{g}$  of D-luciferin. Images show representative mice before and after sacrifice. Right: Plain photographs of the same animals. Metastatic lesions are indicated with arrows. L, liver; S, spleen; T, primary tumor; H/L, heart and lung. (B) The number of metastatic nodules in each group. (C) Weight of the primary tumors from animals sacrificed at day 27.

**Table 1. Number of metastatic lesions in organs.** Nude mice with orthotopic colon cancer (HCT116-luc2) were sacrificed at day 27 after transplantation.

	PBS ( $n = 7$ )	SLpEmpty ( $n = 6$ )	SLpFlaB ( $n = 8$ )
Liver	13	4	0
Spleen	3	0	0
Lung	2	1	0
Mesentery/ intestine	44	15	3
Peritoneal wall	29	6	1
Total	91	26	4
Average	13.0	4.3	0.5

received an intravenous injection of  $\Delta\text{ppGpp}$  *S. typhimurium* carrying an empty vector ( $1 \times 10^7$  CFU) or  $\Delta\text{ppGpp}$  *S. typhimurium* carrying pFlaB ( $1 \times 10^7$  CFU) via the tail vein, in the latter case followed by  $\text{l-arabinose}$  administration at 3 dpi. FlaB-secreting *Salmonella* therapy showed strong therapeutic efficacy in WT mice bearing MC38 tumors, but antitumor activity was completely abrogated in  $\text{TLR4}^{-/-}$  and  $\text{MyD88}^{-/-}$  and partly in  $\text{TLR5}^{-/-}$  mice (Fig. 5, A and B). For example, at day 9 after treatment, the mean tumor volume in WT mice shrank

to 12% of that at the beginning of treatment, whereas in  $\text{TLR4}^{-/-}$  and  $\text{MyD88}^{-/-}$  mice, the tumor volume was 837 and 951% of that at the beginning of treatment, respectively, and was not significantly different from the PBS group (1003%). Tumor growth in  $\text{TLR5}^{-/-}$  mice was moderately suppressed (to 413%; Fig. 5A). Next, we examined the antitumor activity of *S. typhimurium* without a payload ( $\Delta\text{ppGpp}$  *S. typhimurium* carrying an empty vector) in WT,  $\text{TLR4}^{-/-}$ ,  $\text{TLR5}^{-/-}$ , and  $\text{MyD88}^{-/-}$  mice. The same pattern of antitumor activity was observed, such that antitumor activity was completely abrogated in  $\text{TLR4}^{-/-}$  and  $\text{MyD88}^{-/-}$  mice, but some activity remained in  $\text{TLR5}^{-/-}$  mice (Fig. 5C and fig. S12). This finding implies that the TLR4 pathway is a prerequisite for FlaB-mediated anticancer immunity, and the FlaB/TLR5 pathway should synergistically reinforce the tumor-suppressive effects. Immunofluorescence staining revealed that, when compared with WT mice,  $\text{TLR4}^{-/-}$  tumor-bearing mice failed to recruit monocytes/macrophages and neutrophils after bacterial colonization (fig. S13). These results suggest that attenuated *Salmonella* by itself stimulates the host TLR4/MyD88 signaling pathway and sets up a microenvironment in which TLR5 signaling enhances host antitumor responses.

### Phenotypic shifting of tumor macrophages after treatment with FlaB-expressing bacteria

Finally, we examined the functional polarization of macrophages in the tumor microenvironment. The engrafted MC38 tumor tissues were removed from C57BL/6 WT mice 24 hours after induction of FlaB and triple-stained with CD45, F4/80, and CD206 (to detect M2-type macrophages) or with CD45, F4/80, and CD86 (to detect M1-type macrophages) (32, 33). Fluorescence-activated cell sorting

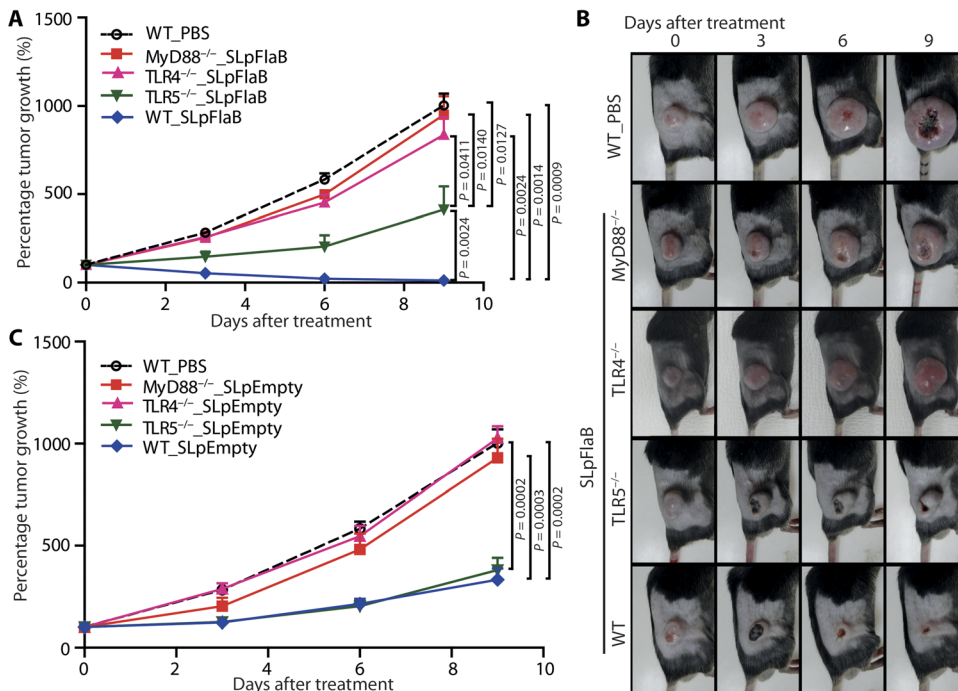


**Fig. 5. Effect of engineered FlaB-secreting *Salmonella* on tumor growth in knockout mice.** C57BL/6 mice (WT, TLR4<sup>-/-</sup>, TLR5<sup>-/-</sup>, and MyD88<sup>-/-</sup>;  $n = 8$  per group) subcutaneously bore MC38 tumors. When the tumors reached a volume of about 120 mm<sup>3</sup>, mice received SLpFlaB ( $1 \times 10^7$  CFU) or PBS via intravenous injection, followed by daily administration of 0.12 g of L-arabinose at 3 dpi. **(A)** Percentage tumor growth after treatment with FlaB-expressing bacteria.  $P$  (WT\_PBS versus MyD88<sup>-/-</sup>\_SLpFlaB) = 1.000;  $P$  (WT\_PBS versus TLR4<sup>-/-</sup>\_SLpFlaB) = 0.3450. **(B)** Photographs of subcutaneous tumors in representative mice. **(C)** Percentage tumor growth after treatment with *Salmonella* carrying an empty vector (SLpEmpty).  $P$  (WT\_PBS versus MyD88<sup>-/-</sup>\_SLpEmpty) = 0.7758;  $P$  (WT\_PBS versus TLR4<sup>-/-</sup>\_SLpEmpty) = 0.6943;  $P$  (WT\_PBS versus TLR5<sup>-/-</sup>\_SLpEmpty) = 0.5054.

(FACS) analysis revealed that CD206<sup>+</sup> M2-like macrophages were more abundant in tumor tissues before bacterial colonization. However, after tumor infiltration by bacteria, the percentage of M2-type macrophages decreased, whereas that of CD86<sup>+</sup> M1-type macrophages increased. This change was more pronounced when the tumor-infiltrating *Salmonella* secreted FlaB (Fig. 6A). This finding was further supported by quadruple staining, which clearly showed an increase in the population of M1-like macrophages in the tumor tissue from mice treated by FlaB-secreting bacteria (fig. S14), and also by double-staining immunofluorescence confocal microscopy (Fig. 6B). The tumor infiltration by bacteria evidently affected M1/M2 polarization. The M2-to-M1 shift was markedly increased upon secretion of FlaB within the tumor microenvironment. The shift was also accompanied by increased secretion of antitumor cytokines (IL-1 $\beta$  and TNF- $\alpha$ ) (fig. S15). To further explore the mechanism underlying tumor necrosis induced by M1-shifted macrophages, we assessed the amount of nitric oxide (NO) in tumor lysates. We found that the amount of NO in tumor tissues containing FlaB-secreting bacteria was significantly higher than in tissue that contained bacteria only or FlaB only ( $P < 0.0001$ ; Fig. 6C). Together, these results suggest that FlaB-expressing bacteria induce M1-like macrophage polarization; these macrophages should then suppress tumor growth by secreting tumor-suppressive cytokines and NO.

## DISCUSSION

Here, FlaB-secreting *Salmonella* targeted to the tumor microenvironment exerted enhanced tumor-suppressive effects through two-step activation

of TLR4 and TLR5 signaling pathways. First, bacterial colonization of tumors increased infiltration and activation of immune cells (5, 27, 34, 35), which appeared to be mediated through TLR4 signaling. Monocyte/macrophage and neutrophil infiltration of bacteria-colonized tumors in TLR4<sup>-/-</sup> mice was lower than in WT mice. Second, the recruited immune cells were likely further activated by the TLR5 signaling triggered by in situ-secreted FlaB in the same microenvironment. These activated effector cells should be able to kill tumor cells by producing cytotoxic mediators, including reactive oxygen species, NO, proteases, membrane-perforating agents, and cytokines (27, 28, 36). We observed higher amounts of IL-1 $\beta$ , TNF- $\alpha$ , and NO in tumor tissues after the FlaB-secreting *S. typhimurium* colonized the tumor microenvironment. The tumor-suppressive effect of FlaB-secreting *Salmonella* was far more potent than that mediated by *Salmonella* harboring an empty vector. A mimicry approach using intravenous injection of *Salmonella* and multiple intratumoral injections of FlaB had a therapeutic effect similar to that of FlaB-secreting *Salmonella*.

Because of accumulating reports that activating various TLRs resulted in anti-tumor effects (31, 37–41), many TLR-specific agonists are currently being investigated for tumor immunotherapy (37). In particular, the antitumor activity of microbe-derived therapeutics has been linked to their ability to activate TLRs. Coley's toxin (an antitumor treatment consisting of a mixture of bacterial toxins from *Streptococcus pyogenes* and *Serratia marcescens*) and OK-432 (a lyophilized preparation of group A *Streptococcus* that has been used to treat cervical, gastric, and oral squamous cell carcinoma) both stimulate TLR4 (41). *Mycobacterium bovis* bacillus Calmette-Guérin, which has been used for 30 years in bladder cancer, is a potent activator of TLR2 and TLR4 (39). MyD88 is a common adaptor molecule for TLRs (except for TLR3), and blocking it should obliterate most TLR signaling relays. Here, we observed that the antitumor effects of FlaB-secreting *Salmonella* were abrogated to a greater extent in TLR4<sup>-/-</sup> and MyD88<sup>-/-</sup> mice than in TLR5<sup>-/-</sup> mice. TLR4 signaling triggered by infiltrating bacterial cells not yet fully expressing FlaB should have induced chemotaxis of neutrophils, monocytes/macrophages, and dendritic cells (DCs). TLR4-mediated immune cell recruitment is expected to be a requisite for the tumor-suppressive activities of FlaB-secreting *Salmonella* because TLR4<sup>-/-</sup> mice were nonresponsive, but TLR5<sup>-/-</sup> mice were partially responsive to the therapy. A number of previous studies support our hypothesis, which demonstrates a relationship between TLR4 signaling and immune cell recruitment (38–40). For example, TLR4 signaling by tissue macrophages or tumor cells induces production of chemokines that promote recruitment of neutrophils (40) or immature DCs (38, 39) to tumors.

The TLR5-expressing population of infiltrating or tissue-resident inflammatory cells may mediate the M2-to-M1 shift observed in tumor



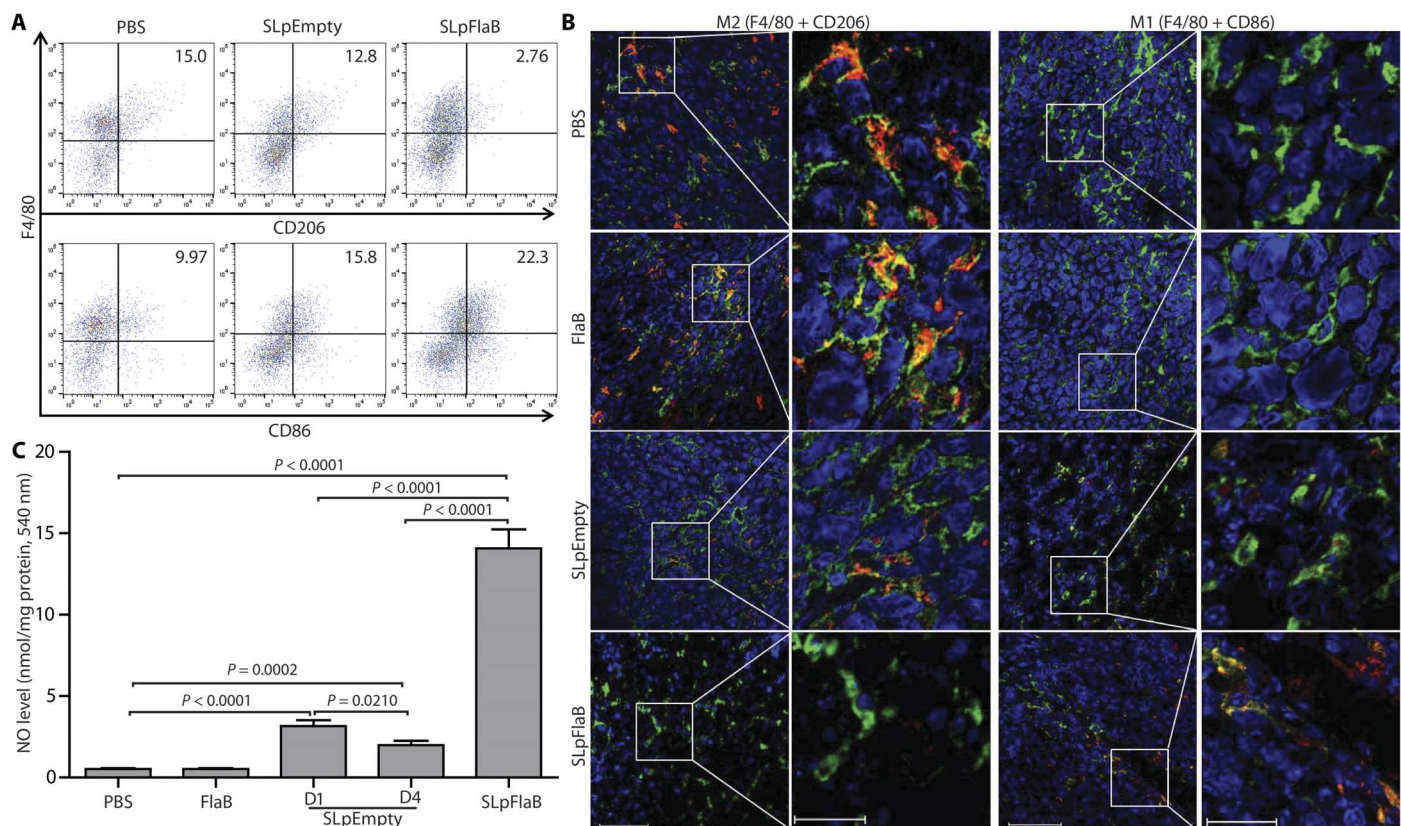


**Fig. 6. M1 and M2 macrophage polarization after treatment with FlaB-secreting bacteria.** Samples were prepared from MC38 tumors 24 hours after induction. **(A)** Samples were triple-stained with CD45 (hematopoietic cell marker), F4/80 (macrophage marker), and CD206 (M2-type macrophages) or CD86 (M1-type macrophages) and analyzed by FACS. All the samples were pregated on CD45-positive cells ( $n = 5$ ; data are representative of three independent experiments). **(B)** Contiguous sections were double-stained with F4/80 (green) and CD206 (red) (M2 macrophage) or F4/80 (green) and CD86 (red) (M1 macrophage). Nuclei were stained with DAPI (blue). A merged image is shown at low (scale bars, 50  $\mu$ m) and high (scale bars, 20  $\mu$ m) magnification. Data are representative of three individual experiments. **(C)** NO concentrations were measured in tumor lysates ( $n = 13$ ) at 1 dpi (D1) and 4 dpi (D4) of SLpEmpty and 4 days after treatment with PBS, FlaB, or SLpFlaB (24 hours after induction).

macrophages after activating NF- $\kappa$ B (42). For example, NF- $\kappa$ B activation in M1 macrophages is critical for tumor-promoting inflammation during the early phase of tumorigenesis. However, during later phases, macrophages are reprogrammed to tumor-associated macrophage or M2-like phenotypes, resulting in low levels of NF- $\kappa$ B activation and increased immunosuppressive capacity (43). The engineered bacterial strain used herein may activate NF- $\kappa$ B via dual pathways, TLR4 (via LPS) and TLR5 (via FlaB), to enhance host antitumor immune responses. Future studies will need to identify TLR5<sup>+</sup> cells that specifically respond to FlaB and examine the mechanism(s) underlying the TLR5-mediated M2-to-M1 shifting. The M1/M2 conversion of tissue macrophages remains controversial (42). Knowing the origin of M1 cells present in tumor tissues colonized by FlaB-secreting bacteria may enable deeper understanding of the cellular mechanism underlying the tumor-suppressive effects described herein; for example, there is a need to examine whether preexisting M2-type cells are converted to M1-type cells or precursor inflammatory monocytes are activated to M1-type cells.

We also found that  $\Delta$ ppGpp *Salmonella*-derived endogenous flagellin was not sufficiently potent to activate tumor-suppressive TLR5 signaling. Bacterial flagellin is the natural ligand for TLR5, and reports indicate that activation of the TLR5 signaling pathway by flagellin induces antitumor activity in several experimental animal models (26, 31, 44). Because flagellin monomers bind to TLR5 (45), endogenous

flagellin molecules assembled into the flagellum structure of *Salmonella* would have less chance to stimulate the TLR5 signaling pathway. Over-produced FlaB being secreted to the microenvironment should have exerted dominant effects. FlaB was more potent in stimulating TLR5 signaling than *Salmonella* flagellin FlhC (25).

Engineered FlaB-expressing bacteria also exerted an antitumor effect in nude mice bearing orthotopic human colon (HCT116-luc2) tumors. The bacteria suppressed both metastasis and growth of the primary orthotopic tumor, presumably because of increased expression of tumor-inhibiting cytokines. In particular, treatment with FlaB-secreting *S. typhimurium* significantly reduced metastasis ( $P = 0.0022$ ). Because nude mice lack T lymphocytes, which are essential for tumor-specific adaptive immunity, this inhibitory effect on metastasis is likely a result of the reduced local tumor burden and altered innate immune status within the tumor microenvironment. Altered inflammatory cell infiltration and cytokine production patterns in tumors colonized by FlaB-secreting *Salmonella* strongly suggest that the orthotopic tumor microenvironment was modulated by the treatment. In the future, systems biological analysis of the tumor microenvironment should provide more information about the underlying cellular and biochemical mechanisms.

Bacterial toxicity is the major barrier to safety and regulatory approval. Therefore, safety concerns regarding BCT need to be addressed. Bacteria administered via the tail vein initially and transiently localized

in reticuloendothelial organs; therefore, cytotoxic agents should be introduced only when the bacteria have been cleared from reticuloendothelial organs and have accumulated in the targeted tumor tissue. Here, this occurred 3 days after bacteria administration. Avoidance of systemic toxicity is the main reason for our use of an inducible promoter in the present study. Early induction of FlaB expression (0 dpi) induced hepatic toxicity owing to high numbers of transient bacteria in the reticuloendothelial system (liver and spleen) (5). However, when FlaB expression was induced starting at 3 dpi, we found that clinical laboratory parameters remained within the normal range, suggesting the absence of any serious inflammation, sepsis, or renal/liver dysfunction. Our *in vivo* experiments indicate that the engineered bacteria have a good safety profile and are, therefore, a promising anticancer agent.

In summary, FlaB-secreting *Salmonella* show excellent anticancer effects in diverse mouse tumor models, suggesting that this strategy could be applied to a wide spectrum of malignancies. In contrast to previous studies that showed that flagellin-mediated cancer therapy was dependent on the presence of TLR5 on the cancer cell surface, we found that the strategy described herein is not restricted to TLR5-expressing cancer cells (31). Here, we primarily described biological mechanisms underlying the anticancer activities of FlaB-secreting *Salmonella* using colorectal tumor cell lines (the strategy worked comparably well with a melanoma model). These effects were mediated through the activation of TLR4 and TLR5 signaling pathways in host immune cells. This approach is based on the cooperative activity of AppGpp *S. typhimurium* and its payload, FlaB, combined with the finding that bacterial colonization and proliferation in tumors strongly induced tumor infiltration and subsequent activation of immune cells. This, coupled with localized production of FlaB, activates a powerful anticancer immune reaction.

## MATERIALS AND METHODS

### Study design

The objective of the study was to develop a strategy for targeted cancer immunotherapy using an engineered *S. typhimurium* strain secreting FlaB, which would enhance host immune system activation at the desired time and location. TLR5-negative cancer cells were used to test whether the FlaB-mediated effects were the consequences of host TLR5 signaling. The bacterial delivery vector AppGpp *S. typhimurium* was transformed with the engineered plasmid pFlaB. Bacterial colonization of tumor tissues was then measured by examining viable bacterial counts and by bioluminescence imaging. FlaB expression *in vivo* was confirmed by quantitative RT-PCR and immunofluorescence staining. The therapeutic efficacy of the engineered bacteria was evaluated in murine xenograft models. Therapeutic efficacy was also compared in C57BL/6 WT, TLR4<sup>-/-</sup>, TLR5<sup>-/-</sup>, and MyD88<sup>-/-</sup> mice to determine whether the antitumor effect of FlaB-secreting bacteria was mediated through host TLR signaling. Polarization of M1-like macrophages was examined by FACS analysis and immunofluorescence staining and by measuring the concentrations of NO and tumor inhibitory cytokines by enzyme-linked immunosorbent assay. Systemic toxicity induced by BCT was examined by measuring clinical chemistry parameters.

### Plasmid and bacterial strain

To engineer FlaB-expressing bacteria, the *flaB* gene (1134 base pairs) was amplified from the *pTYB12-FlaB* plasmid (25) using the following primers: forward, CCATGGCCATGGCAGTGAATGTAAATACA-AACGCAGCAATGAC; reverse, GTTTAACTTAGCCTAGTA-

GACTTAGCGCTGAGTTTGG. Amplified DNA was cut with Nco I and Pme I and used to directly replace *Rluc8* at the same site in pBAD-pelB-*Rluc8* (29). The resulting plasmid was named pFlaB. The empty vector (control) was generated by removing *Rluc8* from pBAD-*Rluc8* and named pEmpty. The bacterial delivery vector AppGpp *S. typhimurium* strain SHJ2037 (*relA::cat*, *spoT::kan*) was reported previously (table S1) (46). Plasmids pFlaB and pEmpty (both harboring an ampicillin resistance gene) were transferred into AppGpp *Salmonella* by electroporation (1.8 kV; Bio-Rad). The new strains were maintained in ampicillin-containing medium and kept in a deep freezer at -80°C as 25% glycerol stocks.

### Animal models

Male C57BL/6 and BALB/c athymic nu<sup>-</sup>/nu<sup>-</sup> mice (5 to 6 weeks old, 18 to 25 g) were purchased from the Orient Company. TLR4<sup>-/-</sup>, TLR5<sup>-/-</sup>, and MyD88<sup>-/-</sup> knockout mice with a C57BL/6 genetic background were described previously (47, 48). All experiments and euthanasia procedures were performed in accordance with protocols approved by the Chonnam National University Animal Research Committee (Gwangju, Republic of Korea). Mice were anesthetized with 2% isoflurane (for tumor assessment) or a mixture of ketamine (200 mg/kg) and xylazine (10 mg/kg) (for surgery). To generate the mouse cancer models, MC38 (1 × 10<sup>6</sup>) or B1610F (5 × 10<sup>5</sup>) cells were subcutaneously implanted into the right flank. Tumors were measured with a caliper every 3 days from day 5 to day 50. Tumor volume (in cubic millimeters) was calculated using the following formula: (L × H × W)/2, where L is the length, W is the width, and H is the height of the tumor in millimeters. Mice with tumor volumes ≥1500 mm<sup>3</sup> were euthanized according to the guidelines of the Animal Research Committee. The orthotopic human colon cancer model was established by surgical implantation of HCT116-luc2 tumor fragments onto the intestinal wall of BALB/c athymic nu<sup>-</sup>/nu<sup>-</sup> mice, as described previously (49).

### Cell preparation and FACS analysis

Peritoneal macrophages were isolated from specific pathogen-free C57BL/6 male mice, as described previously (50). To check TLR5 expression and location, peritoneal macrophages and tumor cells (MC38 and HCT116-luc2) were treated with or without permeabilization reagent (BD) before incubating with an anti-TLR5 antibody. Single-cell suspensions from tumors were prepared by incubating removed tumor pieces in collagenase D (1.0 mg/ml) (Roche) and deoxyribonuclease I (50 µg/ml) (Roche) for 45 min at 37°C, followed by passing through a 40-µm cell strainer. Samples were incubated with specific fluorochrome-labeled antibodies (table S2) at 4°C for 30 min, and at least 20,000 events were analyzed using a FACSCalibur flow cytometer (BD Biosciences). Data were analyzed using FlowJo (Tree Star) software. The analysis gate was set on the basis of isotype plots. The M1/M2 phenotype analysis in each group was performed using the same gate. Because the background signals in experimental groups were different, which may be due to different degrees of cell injury resulting from the different modes of treatment (PBS, empty *Salmonella*, and FlaB-secreting *Salmonella*), we adjusted gating parameters for the FACS analysis of different groups (51, 52).

### Statistical analysis

Statistical analysis was performed using the GraphPad Prism 5.0 software. Mann-Whitney *U* test was used to determine the statistical significance of differences in tumor growth and mRNA expression between control and treatment groups. A *P* value <0.05 was considered



statistically significant. Survival analysis was performed using the Kaplan-Meier method and the log-rank test. All data are expressed as means  $\pm$  SEM.

## SUPPLEMENTARY MATERIALS

www.sciencetranslationalmedicine.org/cgi/content/full/9/376/eaak9537/DC1

### Materials and Methods

Fig. S1. NF- $\kappa$ B activation by LPS and FlaB in cancer cells and peritoneal macrophages in vitro.

Fig. S2. Luciferase assay in HCT116 cancer cells.

Fig. S3. Spleen weight after *Salmonella* treatment.

Fig. S4. Analysis of cell populations in the spleen after *Salmonella* treatment.

Fig. S5. Noninvasive monitoring of bacterial distribution in vivo.

Fig. S6. Distribution of bacteria in MC38 tumor-bearing mice.

Fig. S7. Detection of bacteria and FlaB in liver and tumor tissues.

Fig. S8. Systemic toxicity of FlaB-expressing bacteria.

Fig. S9. Photographs of mice treated with FlaB-secreting bacteria.

Fig. S10. Antitumor effect in a B16F10 melanoma model.

Fig. S11. Tumor growth in WT and knockout mice.

Fig. S12. Effect of bacterial treatments on tumor growth in TLR4 knockout mice.

Fig. S13. Cell infiltration in WT and knockout mice after *Salmonella* treatment.

Fig. S14. Macrophage polarization after treatment with FlaB-secreting bacteria assessed by quadruple staining.

Fig. S15. Detection of tumor-suppressive cytokines in tumor tissues.

Table S1. Bacterial strains and plasmids used in the study.

Table S2. Antibodies used in the study.

## REFERENCES AND NOTES

- W. Wei, Q. H. Shi, F. Remacle, L. D. Qin, D. B. Shackelford, Y. S. Shin, P. S. Mischel, R. D. Levine, J. R. Heath, Hypoxia induces a phase transition within a kinase signaling network in cancer cells. *Proc. Natl. Acad. Sci. U.S.A.* **110**, E1352–E1360 (2013).
- J. M. Brown, W. R. William, Exploiting tumour hypoxia in cancer treatment. *Nat. Rev. Cancer* **4**, 437–447 (2004).
- H. Zhu, Z. Li, S. Mao, B. Ma, S. Zhou, L. Deng, T. Liu, D. Cui, Y. Zhao, J. He, C. Yi, Y. Huang, Antitumor effect of sFlt-1 gene therapy system mediated by *Bifidobacterium Infantis* on Lewis lung cancer in mice. *Cancer Gene Ther.* **18**, 884–896 (2011).
- M. Zhao, M. Yang, X. M. Li, P. Jiang, E. Baranov, S. Li, M. Xu, S. Penman, R. M. Hoffman, Tumor-targeting bacterial therapy with amino acid auxotrophs of GFP-expressing *Salmonella typhimurium*. *Proc. Natl. Acad. Sci. U.S.A.* **102**, 755–760 (2005).
- S. N. Jiang, S. H. Park, H. J. Lee, J. H. Zheng, H. S. Kim, H. S. Bom, Y. Hong, M. Szardenings, M. G. Shin, S. C. Kim, V. Ntziachristos, H. E. Choy, J. J. Min, Engineering of bacteria for the visualization of targeted delivery of a cytolytic anticancer agent. *Mol. Ther.* **21**, 1985–1995 (2013).
- J.-J. Min, V. H. Nguyen, H.-J. Kim, Y. Hong, H. E. Choy, Quantitative bioluminescence imaging of tumor-targeting bacteria in living animals. *Nat. Protoc.* **3**, 629–636 (2008).
- S. N. Jiang, T. X. Phan, T. K. Nam, V. H. Nguyen, H. S. Kim, H. S. Bom, H. E. Choy, Y. Hong, J.-J. Min, Inhibition of tumor growth and metastasis by a combination of *Escherichia coli*-mediated cytolytic therapy and radiotherapy. *Mol. Ther.* **18**, 635–642 (2010).
- N. J. Roberts, L. Zhang, F. Janku, A. Collins, R.-Y. Bai, V. Staedtke, A. W. Rusk, D. Tung, M. Miller, J. Roix, K. V. Khanna, R. Murthy, R. S. Benjamin, T. Helgason, A. D. Szvalb, J. E. Bird, S. Roy-Chowdhuri, H. H. Zhang, Y. Qiao, B. Karim, J. McDaniel, A. Elpiner, A. Sahara, J. Lachowicz, B. Phillips, A. Turner, M. K. Klein, G. Post, L. A. Diaz Jr., G. J. Riggins, N. Papadopoulos, K. W. Kinzler, B. Vogelstein, C. Bettgowda, D. L. Huso, M. Varterasian, S. Saha, S. Zhou, Intratumoral injection of *Clostridium novyi*-NT spores induces antitumor responses. *Sci. Transl. Med.* **6**, 249ra111 (2014).
- D. Akin, J. Sturgis, K. Ragheb, D. Sherman, K. Burkholder, J. P. Robinson, A. K. Bhunia, S. Mohammed, R. Bashir, Bacteria-mediated delivery of nanoparticles and cargo into cells. *Nat. Nanotechnol.* **2**, 441–449 (2007).
- C. Clairmont, K. C. Lee, J. Pike, M. Ittensohn, K. B. Low, J. Pawelek, D. Bermudes, S. M. Brecher, D. Margitich, J. Turnier, Z. Li, X. Luo, I. King, L. M. Zheng, Biodistribution and genetic stability of the novel antitumor agent VNP20009, a genetically modified strain of *Salmonella typhimurium*. *J. Infect. Dis.* **181**, 1996–2002 (2000).
- P. Chorobik, D. Czapllicki, K. Ossysek, J. Bereta, *Salmonella* and cancer: From pathogens to therapeutics. *Acta Biochim. Pol.* **60**, 285–297 (2013).
- J. F. Toso, V. J. Gill, P. Hwu, F. M. Marincola, N. P. Restifo, D. J. Schwartzentruber, R. M. Sherry, S. L. Topalian, J. C. Yang, F. Stock, L. J. Freezer, K. E. Morton, C. Seipp, L. Haworth, S. Mavroukakis, D. White, S. MacDonald, J. Mao, M. Sznol, S. A. Rosenberg, Phase I study of the intravenous administration of attenuated *Salmonella typhimurium* to patients with metastatic melanoma. *J. Clin. Oncol.* **20**, 142–152 (2002).
- C. Yam, M. Zhao, K. Hayashi, H. Y. Ma, H. Kishimoto, M. McElroy, M. Bouvet, R. M. Hoffman, Monotherapy with a tumor-targeting mutant of *S. typhimurium* Inhibits liver metastasis in a mouse model of pancreatic cancer. *J. Surg. Res.* **164**, 248–255 (2010).
- M. Zhao, M. Yang, H. Y. Ma, X. M. Li, X. Y. Tan, S. K. Li, Z. J. Yang, R. M. Hoffman, Targeted therapy with a *Salmonella typhimurium* leucine-arginine auxotroph cures orthotopic human breast tumors in nude mice. *Cancer Res.* **66**, 7647–7652 (2006).
- M. Zhao, J. Geller, H. Ma, M. Yang, S. Penman, R. M. Hoffman, Monotherapy with a tumor-targeting mutant of *Salmonella typhimurium* cures orthotopic metastatic mouse models of human prostate cancer. *Proc. Natl. Acad. Sci. U.S.A.* **104**, 10170–10174 (2007).
- S. Yano, Y. Zhang, M. Zhao, Y. Hiroshima, S. Miwa, F. Uehara, H. Kishimoto, H. Tazawa, M. Bouvet, T. Fujiwara, R. M. Hoffman, Tumor-targeting *Salmonella typhimurium* A1-R decoys quiescent cancer cells to cycle as visualized by FUCI imaging and become sensitive to chemotherapy. *Cell Cycle* **13**, 3958–3963 (2014).
- H. S. Na, H. J. Kim, H.-C. Lee, Y. Hong, J. H. Rhee, H. E. Choy, Immune response induced by *Salmonella typhimurium* defective in ppGpp synthesis. *Vaccine* **24**, 2027–2034 (2006).
- V. H. Nguyen, H.-S. Kim, J.-M. Ha, Y. J. Hong, H. E. Choy, J.-J. Min, Genetically engineered *Salmonella typhimurium* as an imageable therapeutic probe for cancer. *Cancer Res.* **70**, 18–23 (2010).
- J.-H. Jeong, K. Kim, D. Lim, K. Jeong, Y. Hong, V. H. Nguyen, T.-H. Kim, S. Ryu, J.-A. Lim, J. I. Kim, G.-J. Kim, S. C. Kim, J.-J. Min, H. E. Choy, Anti-tumoral effect of the mitochondrial target domain of Noxa delivered by an engineered *Salmonella typhimurium*. *PLOS ONE* **9**, e80050 (2014).
- M. Loeffler, G. Le'Negrate, M. Krajewska, J. C. Reed, IL-18-producing *Salmonella* inhibit tumor growth. *Cancer Gene Ther.* **15**, 787–794 (2008).
- H. Nishikawa, E. Sato, G. Briones, L.-M. Chen, M. Matsuo, Y. Nagata, G. Ritter, E. Jager, H. Nomura, S. Kondo, I. Tawara, T. Kato, H. Shiku, L. J. Old, J. E. Galán, S. Gnajic, In vivo antigen delivery by a *Salmonella typhimurium* type III secretion system for therapeutic cancer vaccines. *J. Clin. Invest.* **116**, 1946–1954 (2006).
- C. Grillot-Courvalin, S. Goussard, F. Huetz, D. M. Ojcius, P. Courvalin, Functional gene transfer from intracellular bacteria to mammalian cells. *Nat. Biotechnol.* **16**, 862–866 (1998).
- M. Loeffler, G. Le'Negrate, M. Krajewska, J. C. Reed, Attenuated *Salmonella* engineered to produce human cytokine LIGHT inhibit tumor growth. *Proc. Natl. Acad. Sci. U.S.A.* **104**, 12879–12883 (2007).
- M. Loeffler, G. Le'Negrate, M. Krajewska, J. C. Reed, *Salmonella typhimurium* engineered to produce CCL21 inhibit tumor growth. *Cancer Immunol. Immunother.* **58**, 769–775 (2009).
- S. E. Lee, S. Y. Kim, B. C. Jeong, Y. R. Kim, S. J. Bae, O. S. Ahn, J.-J. Lee, H.-C. Song, J. M. Kim, H. E. Choy, S. S. Chung, M.-N. Kwon, J. H. Rhee, A bacterial flagellin, *Vibrio vulnificus* FlaB, has a strong mucosal adjuvant activity to induce protective immunity. *Infect. Immun.* **74**, 694–702 (2006).
- C. T. Nguyen, S. H. Hong, J.-I. Sin, H. V. D. Vu, K. Jeong, K. O. Cho, S. Uematsu, S. Akira, S. E. Lee, J. H. Rhee, Flagellin enhances tumor-specific CD8<sup>+</sup> T cell immune responses through TLR5 stimulation in a therapeutic cancer vaccine model. *Vaccine* **31**, 3879–3887 (2013).
- J.-E. Kim, T. X. Phan, V. H. Nguyen, H.-V. Dinh-Vu, J. H. Zheng, M. Yun, S.-G. Park, Y. Hong, H. E. Choy, M. Szardenings, W. Hwang, J.-A. Park, S. Park, S.-H. Im, J.-J. Min, *Salmonella typhimurium* suppresses tumor growth via the pro-inflammatory cytokine interleukin-1 $\beta$ . *Theranostics* **5**, 1328–1342 (2015).
- T. X. Phan, V. H. Nguyen, M. T.-Q. Duong, Y. Hong, H. E. Choy, J.-J. Min, Activation of inflammasome by attenuated *Salmonella typhimurium* in bacteria-mediated cancer therapy. *Microbiol. Immunol.* **59**, 664–675 (2015).
- U. N. Le, H.-S. Kim, J.-S. Kwon, M. Y. Kim, V. H. Nguyen, S. N. Jiang, B.-I. Lee, Y. Hong, M. G. Shin, J. H. Rhee, H.-S. Bom, Y. Ahn, S. S. Gambhir, H. E. Choy, J.-J. Min, Engineering and visualization of bacteria for targeting infarcted myocardium. *Mol. Ther.* **19**, 951–959 (2011).
- S.-P. Lei, H.-C. Lin, S.-S. Wang, J. Callaway, G. Wilcox, Characterization of the *Erwinia carotovora pelB* gene and its product pectate lyase. *J. Bacteriol.* **169**, 4379–4383 (1987).
- Z. Y. Cai, A. Sanchez, Z. C. Shi, T. T. Zhang, M. Y. Liu, D. K. Zhang, Activation of Toll-like receptor 5 on breast cancer cells by flagellin suppresses cell proliferation and tumor growth. *Cancer Res.* **71**, 2466–2475 (2011).
- X. Xiao, I. Gaffar, P. Guo, J. Wiersch, S. Fischbach, L. Peirish, Z. Song, Y. El-Gohary, K. Prasad, C. Shiota, G. K. Gittes, M2 macrophages promote beta-cell proliferation by up-regulation of SMAD7. *Proc. Natl. Acad. Sci. U.S.A.* **111**, E1211–E1220 (2014).
- K. A. Kigerl, J. C. Gensel, D. P. Ankeny, J. K. Alexander, D. J. Donnelly, P. G. Popovich, Identification of two distinct macrophage subsets with divergent effects causing either neurotoxicity or regeneration in the injured mouse spinal cord. *J. Neurosci.* **29**, 13435–13444 (2009).
- C.-H. Lee, C.-L. Wu, A.-L. Shiau, Toll-like receptor 4 mediates an antitumor host response induced by *Salmonella choleraesuis*. *Clin. Cancer Res.* **14**, 1905–1912 (2008).
- C.-H. Lee, C.-L. Wu, A.-L. Shiau, *Salmonella choleraesuis* as an anticancer agent in a syngeneic model of orthotopic hepatocellular carcinoma. *Int J Cancer* **122**, 930–935 (2008).

36. E. Di Carlo, G. Forni, P. Lollini, M. P. Colombo, A. Modesti, P. Musiani, The intriguing role of polymorphonuclear neutrophils in antitumor reactions. *Blood* **97**, 339–345 (2001).
37. H. Kanzler, F. J. Barrat, E. M. Hessel, R. L. Coffman, Therapeutic targeting of innate immunity with Toll-like receptor agonists and antagonists. *Nat. Med.* **13**, 552–559 (2007).
38. L. Wang, Q. Liu, Q. Sun, C. Zhang, T. Chen, X. Cao, TLR4 signaling in cancer cells promotes chemoattraction of immature dendritic cells via autocrine CCL20. *Biochem. Biophys. Res. Commun.* **366**, 852–856 (2008).
39. S. Tsuji, M. Matsumoto, O. Takeuchi, S. Akira, I. Azuma, A. Hayashi, K. Toyoshima, T. Seya, Maturation of human dendritic cells by cell wall skeleton of *Mycobacterium bovis* bacillus Calmette-Guérin: Involvement of Toll-like receptors. *Infect. Immun.* **68**, 6883–6890 (2000).
40. K. De Filippo, R. B. Henderson, M. Laschinger, N. Hogg, Neutrophil chemokines KC and macrophage-inflammatory protein-2 are newly synthesized by tissue macrophages using distinct TLR signaling pathways. *J. Immunol.* **180**, 4308–4315 (2008).
41. S. Rakoff-Nahoum, R. Medzhitov, Toll-like receptors and cancer. *Nat. Rev. Cancer* **9**, 57–63 (2009).
42. N. Wang, H. Liang, K. Zen, Molecular mechanisms that influence the macrophage M1–M2 polarization balance. *Front. Immunol.* **5**, 614 (2014).
43. S. K. Biswas, L. Gangi, S. Paul, T. Schioppa, A. Sacconi, M. Sironi, B. Bottazzi, A. Doni, B. Vincenzo, F. Pasqualini, L. Vago, M. Nebuloni, A. Mantovani, A. Sica, A distinct and unique transcriptional program expressed by tumor-associated macrophages (defective NF- $\kappa$ B and enhanced IRF-3/STAT1 activation). *Blood* **107**, 2112–2122 (2006).
44. L. Sfondrini, A. Rossini, D. Besusso, A. Merlo, E. Tagliabue, S. Mènard, A. Balsari, Antitumor activity of the TLR-5 ligand flagellin in mouse models of cancer. *J. Immunol.* **176**, 6624–6630 (2006).
45. J.-M. Reichhart, TLR5 takes aim at bacterial propeller. *Nat. Immunol.* **4**, 1159–1160 (2003).
46. M. Y. Song, H. J. Kim, E. Y. Kim, M. S. Shin, H. C. Lee, Y. J. Hong, J. H. Rhee, H. Yoon, S. Ryu, S. Lim, H. E. Choy, ppGpp-dependent stationary phase induction of genes on *Salmonella* pathogenicity island 1. *J. Biol. Chem.* **279**, 34183–34190 (2004).
47. S. Uematsu, M. H. Jang, N. Chevrier, Z. Guo, Y. Kumagai, M. Yamamoto, H. Kato, N. Sougawa, H. Matsui, H. Kuwata, H. Hemmi, C. Coban, T. Kawai, K. J. Ishii, O. Takeuchi, M. Miyasaka, K. Takeda, S. Akira, Detection of pathogenic intestinal bacteria by Toll-like receptor 5 on intestinal CD11c<sup>+</sup> lamina propria cells. *Nat. Immunol.* **7**, 868–874 (2006).
48. O. Adachi, T. Kawai, K. Takeda, M. Matsumoto, H. Tsutsui, M. Sakagami, K. Nakanishi, S. Akira, Targeted disruption of the *MyD88* gene results in loss of il-1- and il-18-mediated function. *Immunity* **9**, 143–150 (1998).
49. A. Rajput, I. Dominguez San Martin, R. Rose, A. Beko, C. LeVea, E. Sharratt, R. Mazurchuk, R. M. Hoffman, M. G. Brattain, J. Wang, Characterization of HCT116 human colon cancer cells in an orthotopic model. *J. Surg. Res.* **147**, 276–281 (2008).
50. X. Zhang, R. Goncalves, D. M. Mosser, The isolation and characterization of murine macrophages. *Curr. Protoc. Immunol.* 10.1002/0471142735.im1401s83 (2008).
51. T. Saito, H. Nishikawa, H. Wada, Y. Nagano, D. Sugiyama, K. Atarashi, Y. Maeda, M. Hamaguchi, N. Ohkura, E. Sato, H. Nagase, J. Nishimura, H. Yamamoto, S. Takiguchi, T. Tanoue, W. Suda, H. Morita, M. Hattori, K. Honda, M. Mori, Y. Doki, S. Sakaguchi, Two FOXP3<sup>+</sup>CD4<sup>+</sup> T cell subpopulations distinctly control the prognosis of colorectal cancers. *Nat. Med.* **22**, 679–684 (2016).
52. O. A. Ali, D. Emerich, G. Dranoff, D. J. Mooney, In situ regulation of DC subsets and T cells mediates tumor regression in mice. *Sci. Transl. Med.* **1**, 8ra19 (2009).

**Acknowledgments:** We thank J.-J. Lee for providing the MC38 cell line. **Funding:** This work was supported by the Pioneer Research Center Program (2015M3C1A3056410) and the Bio & Medical Technology Development Program (NRF-2014M3A9B5073747) of the National Research Foundation of Korea (NRF), funded by the Ministry of Science, ICT and Future Planning. H.E.C. was supported by the NRF (no. 2012-0006072). J.H.R. was supported by a grant of the Korean Health Technology R&D Project through the Korea Health Industry Development Institute, funded by the Ministry of Health and Welfare, Republic of Korea (no. HI14C0187). S.-N.J. was supported by the Science and Technology program (ZDXM20130067) from Hainan, China. **Author contributions:** J.H.Z. performed the experiments, analyzed the data, drafted the figures, and co-wrote the manuscript. V.H.N. developed and performed immunofluorescence staining. S.-N.J. and W.T. assisted with the animal experiments. S.-H.P., Y.H., H.-S.B., and H.E.C. analyzed and discussed the data. S.H.H. and S.E.L. obtained and analyzed the immunological data. M.G.S. performed the toxicity studies and analyzed the data. I.-J.C. developed the knockout mice. J.H.R. and J.-J.M. conceived the study, supervised the experiments, analyzed the data, and co-wrote the manuscript. **Competing interests:** The authors declare that they have no competing interests.

Submitted 20 September 2016  
 Resubmitted 16 November 2016  
 Accepted 2 December 2016  
 Published 8 February 2017  
 10.1126/scitranslmed.aak9537

**Citation:** J. H. Zheng, V. H. Nguyen, S.-N. Jiang, S.-H. Park, W. Tan, S. H. Hong, M. G. Shin, I.-J. Chung, Y. Hong, H.-S. Bom, H. E. Choy, S. E. Lee, J. H. Rhee, J.-J. Min, Two-step enhanced cancer immunotherapy with engineered *Salmonella typhimurium* secreting heterologous flagellin. *Sci. Transl. Med.* **9**, eaak9537 (2017).

**Two-step enhanced cancer immunotherapy with engineered *Salmonella typhimurium* secreting heterologous flagellin**

Jin Hai Zheng, Vu H. Nguyen, Sheng-Nan Jiang, Seung-Hwan Park, Wenzhi Tan, Seol Hee Hong, Myung Geun Shin, Ik-Joo Chung, Yeongjin Hong, Hee-Seung Bom, Hyon E. Choy, Shee Eun Lee, Joon Haeng Rhee and Jung-Joon Min (February 8, 2017)  
*Science Translational Medicine* **9** (376), . [doi: 10.1126/scitranslmed.aak9537]

Editor's Summary

**Two bacteria can be better than one**

In some cases, injecting tumors with specific bacteria can help eradicate the tumors by stimulating inflammation and triggering an antitumor immune response. A classic example of this is injection of bladder cancer with bacillus Calmette-Guérin, but more recent approaches have used bacteria such as *Clostridium* and *Salmonella* species. Building on the idea of antitumor bacterial therapy, Zheng *et al.* engineered a weakened strain of *Salmonella typhimurium* to produce the flagellin B protein from another bacterium, *Vibrio vulnificus*. The engineered bacteria induced an effective antitumor immune response, successfully treating tumors in several different mouse models with no evidence of toxicity.

---

The following resources related to this article are available online at <http://stm.sciencemag.org>.  
This information is current as of February 20, 2017.

---

<b>Article Tools</b>	Visit the online version of this article to access the personalization and article tools: <a href="http://stm.sciencemag.org/content/9/376/eaak9537">http://stm.sciencemag.org/content/9/376/eaak9537</a>
<b>Supplemental Materials</b>	"Supplementary Materials" <a href="http://stm.sciencemag.org/content/suppl/2017/02/06/9.376.eaak9537.DC1">http://stm.sciencemag.org/content/suppl/2017/02/06/9.376.eaak9537.DC1</a>
<b>Related Content</b>	The editors suggest related resources on <i>Science's</i> sites: <a href="http://stm.sciencemag.org/content/scitransmed/7/289/289ra84.full">http://stm.sciencemag.org/content/scitransmed/7/289/289ra84.full</a> <a href="http://stm.sciencemag.org/content/scitransmed/6/249/249ra111.full">http://stm.sciencemag.org/content/scitransmed/6/249/249ra111.full</a>
<b>Permissions</b>	Obtain information about reproducing this article: <a href="http://www.sciencemag.org/about/permissions.dtl">http://www.sciencemag.org/about/permissions.dtl</a>

*Science Translational Medicine* (print ISSN 1946-6234; online ISSN 1946-6242) is published weekly, except the last week in December, by the American Association for the Advancement of Science, 1200 New York Avenue, NW, Washington, DC 20005. Copyright 2017 by the American Association for the Advancement of Science; all rights reserved. The title *Science Translational Medicine* is a registered trademark of AAAS.